Shahrood University of Technology

Journal of Hydraulic and Water Engineering (JHWE)

Journal homepage: https://jhwe.shahroodut.ac.ir/

Iranian Hydraulic Association (IHA)

An Index to Determine Reaction of Vegetation Canopies to River Flow

S. Salmanzadeh [1,*], M. Fathi-Moghadam [1], J. Ahadiyan [1], M. Sajadi [1]

[1] Faculty of Water and Environmental Engineering, Shahid Chamran University of Ahvaz, Ahvaz, Iran.

Article Info

Article history:

Received: 4 Aug 2023
Received in revised form: 20 Aug 2023
Accepted: 27 Aug 2023
Published online: 28 Aug 2023

DOI:
10.22044/JHWE.2023.13441.1027

Keywords:
Friction Coefficient Coniferous Tree
Mechanics of Tree
Natural Frequency
Resistance to Flow

Abstract

The physical properties of tree species determine their reaction to external loads as a result of water flow. The greater the tree's ability to withstand water load, the greater the amount of water energy absorption, generation of water eddies, and the acceleration of turbulence in vegetation canopies. This will increase water flow energy lost. In general, the physical properties of trees include leaf density, shape, and overall flexibility of their species. In this study, an index is proposed to characterize the physical properties of tree species. This will enable the application of a single momentum (or energy) equation to determine the overall reaction of a variety of tree species in a community. The index is derived based on the resonance frequency of the first mode of vibration of trees and a fundamental relationship for the homogeneous beams. The derived indexes for four species of coniferous trees were used in a mathematical model to estimate the drag and energy coefficients as representatives for tree reaction to water flow and could account for the differences due to the leaf density, shape, and rigidity of the tree species.

1. Introduction

Vegetation canopies such as seagrass meadows, crop fields, and dense forests provide important ecological services by providing habitats for wildlife, capturing suspended sediment, adjusting temperature, and improving water quality through interactions with the fluid flows they grow in. The study of the mechanics of trees probably started with the analysis of a Cambridge mathematician named A.G. Greenhill for the derivation of a relationship between the height and diameter of the trunk (PUGSLEY, 1988). Chenge (2021) investigated the height-diameter relationship of trees in the nature forest reserve and used height-diameter models as an alternative for predicting tree heights. McMahon and Kronauer (1976) found further evidence supporting the conviction expressed in the literature that the branching pattern within any species is approximately stationary. This means that a tree's structure is self-similar so that any patch of the structure is a model of the entire tree and even the whole species. In a more dynamic hypothesis, he suggests that the only way the crown shape could be maintained the same during growth would be to keep the chord angles the same,

* *Corresponding author:* samira.salmanzade@yahoo.com

which is just the condition for elastic similarity. Moreno-Fernández et al. (2018) developed site quality models using the height-diameter relationship as the reference index and incorporating physiographic and climatic variables. Kafuti et al. (2022) measured the height and diameter of 2,288 *Pericopsis elata* trees. The accuracy of multi-species equations in predicting *P. elata* height was examined and a species-specific equation was developed. The effects of stand-level and environmental variables on the allometric equation showed notable variation between sites driven by differences in maximum asymptotic height. Makowski et al. (2019) presented a multi-scale method for designing large-scale ecosystems with realistically modeled individual plants. This approach leverages self-similarities for efficient modeling of plant geometry and adheres to biological priors. The physical and mechanical properties of tree species and their reaction to water flow an important subjects when dealing with the exchange of mass, momentum, and energy (turbulence mixing) between flow and vegetation. Wang et al. (2022) created a 3D numerical model using large-eddy simulation and the immersed boundary method to study the interaction between flow and flexible vegetation with clustered leaves. The results showed that the model effectively simulates velocity profiles and movement of the vegetation induced by the flow. Tree reaction or in fact, resistance to water flow is highly sensitive to the water velocity and its own physical and mechanical condition. The resistance to flow decreases rapidly as the water velocity increases, due to the streamlining and the resulting streamlining and reduction of the frontal area of tree foliage. The fundamental physical and mechanical properties to be considered in establishing a resistance equation are leaf density, shape, flexibility, and manner of defection of the tree species (Aberle and Järvelä, 2013; Järvelä, 2004; Ji et al., 2023; Kouwen and Fathi-Moghadam, 2000; van Wesenbeeck et al., 2022). Tymiński and Kałuża (2012) conducted laboratory tests on willow, reed, and alder branches to determine their mechanical properties including the relation between elasticity and humidity. The results showed that properties varied within samples from a single plant and were dependent on species and humidity. Gosselin (2019) investigated the mechanics of fluid-structure interactions on individual plants including reconfiguration, poroelasticity, torsion, chirality, buoyancy, skin friction, wave action, flutter, and vortex-induced vibrations. Fang et al. (2022) used a fluid-structure modeling approach to investigate the interaction between the unsteady flow above the mixing layer and the vegetation canopy. They explored the dependence of vegetation behavior on bending rigidity and canopy density. Mewis (2021) proposed a new procedure to estimate the hydraulic resistance of vegetation using the Beer-Lambert law to calculate the vegetation density parameter and incorporate it into a flow model.

To develop a single mathematical model to estimate the water load or reaction of all tree species in a community, an index (symbolized as ξE) is required in a particular model to account for the physical properties (i.e., the effects of leaf density, shape, and rigidity) of individual trees. The purpose of this study is to present a practical procedure for estimation of tree index (ξE), and identifying the reaction of a tree species. The resistance coefficients are used in this study to measure tree reaction to water flow. They include the drag force coefficient for the momentum approach and the energy loss coefficient (or in this case the water flow energy transfer coefficient (f) when an energy equation is used to solve a particular problem. These coefficients can easily be derived from one another for a given condition (Fathi-Moghadam et al., 2010). In general, these coefficients are key parameters for estimating the water velocity profile and characterizing turbulent boundary layer flow above and through a vegetation canopy. These are interesting subjects when dealing with the rate of exchange of momentum and energy

between vegetation and vegetation and river flow. The application of natural frequency to determine the mechanical behavior of vegetation is novel in this study. The proposed method is used to estimate a new tree index for four species of coniferous trees including cedar (*Thuja occidentalis*), spruce (*Picea glauca*), white pine (*Pinus strobus*), and Austrian pine (*Pinus palustris*). The calculated indices for four species of coniferous trees were used in a mathematical model developed by Fathi-Moghadam (Fisher and Dawson, 2003) to estimate the drag and energy lost coefficient, and were able to account for the differences due to the leaf density, shape, and rigidity of the tree species.

2. Material and methods

Theoretically, any beam, tree, or plant stem with mass and elasticity may exhibit one or more resonance frequencies of vibration depending on damping (McMahon and Kronauer, 1976; Niklas and Moon, 1988; Timoshenko and Gere, 2009). For small damping, these resonance frequencies are close to the natural frequencies of the beam. Natural frequencies result from the cyclic exchange of kinetic and potential energy when a structure such as a beam or a plant stem is vibrated. The kinetic energy is proportional to the square of the velocity of the structural mass, while the potential energy is proportional to the square of the elastic strains. The rate of exchange between kinetic and potential energy is the natural frequency of vibration.

The resonance frequencies, *fj* (with *j* = *1,2,3,...,n*, where f_1 is the fundamental or base natural frequency and $f_{2,..n}$ are higher modes of natural frequencies) of a linear and homogeneous beam depend upon its length (*l*), mass per unit length (*m*), second moment of inertia (*I*), modulus of elasticity (*E*), as well as a dimensionless parameter (λj), which is a function of beam geometry and the boundary conditions under which the beam is tested. The relationship between the resonance frequencies and the above variables is given by the following equation (Clough and Penzien, 2003; Timoshenko and Gere, 2009):

$$f_j = \frac{\lambda_j^{\,2}}{2\pi}\left(\frac{EI}{ml^4}\right)^{1/2} \quad (1)$$

where *EI* is the flexural stiffness.

The values of (λj) have been theoretically calculated for a variety of beam geometry (i.e. prismatic, non-prismatic, and tapered beams) and methods of attachment (i.e. boundary conditions), which can be found in advanced dynamic and vibration standard texts. Wang and Worley (1966) presented numerically based tables of natural frequencies and nodes for the transverse vibration of tapered beams. The tables cover the whole range of elliptical tapering. The published values for λj, *E*, and *I* can be used in Eq. 1 with sufficient accuracy for linear and homogeneous beams. If the geometry of the beam does not resemble the geometry of the beam presented in the literature, then a model can be constructed with specified dimensions and known material properties, i.e. known *EI*; after measuring *fj*, the value of (λj) can be computed and then used to determine flexural stiffness *EI* for a given beam. Niklas and Moon (1988) measured flexural stiffness and modulus of elasticity of flower stalks using multiple resonance frequency analysis (MRFA) of spectra. The flower stems were attached to a shaker and their vibrations were tracked by an Opteron camera and analyzed by a spectrum analyzer. For small and symmetric shape vegetation elements such as flower stems the use of published *E*, *I*, and λ_j-values in Eq. 1 to estimate a material property may be appropriate. Such a method or methods for simple structures (like beams) are less applicable for large-scale and complex structures like trees.

2.1. Development of a semi-empirical method to index tree species

In classical mechanics of materials, vegetative biomass is classified as a non-homogeneous visco-elastic material (Niklas, 1992). For large trees, this non-homogeneity will be much greater than short grass or analysis of small plant segments. Trees have different classes of branches and notable differences in ratios of hardwood and softwood in their segments. It should be noted that the vegetal drag coefficient for the leafy trees was found to be three to seven times that of the leafless trees (Järvelä, 2004). The complexity and large non-homogeneity of the visco-elastic materials of large trees disqualify the use of theoretical values of E, I, and λ_j to characterize a tree species. This defines a need to derive a semi-empirical relationship based on extensive tests on various tree species for the estimation of tree indices and quantification of the physical properties of species. To avoid errors resulting from the use of theoretically-based values for λj, I, and E in Eq. 1 and to minimize the number of unknowns, several simplifications have been made in this study. The dimensionless ratio of ($I\ l^{-4}$) in Eq. 1 together with the parameter [$\lambda j^2\ (2\pi)^{-1}$] can be assumed to be a single parameter, symbolized as ξ for the base mode of vibration. This parameter characterizes height, mass or leaf density, and the moment of inertia of a tree. Substituting the tree's height (h) for the beam length (l) in Eq. 1 and transferring the measurable parameters to the right side, Eq. 1 for the first mode of the natural frequency (f_1) will be:

$$\xi E = f_1^{\,2}\left(\frac{m_s}{h}\right) \qquad (2)$$

where $m_s = m.\ h$, the total mass of the tree and ξE, is called the "tree index" in this study. Measuring a tree's height, mass, and recording its natural frequency of the first mode of vibration, the tree index can be estimated by Eq. 2. The developed tree index includes all physical and mechanical properties of a tree species for their leaf density, shape, stiffness, and manner of deflection.

2.2. Experiment procedure and apparatus

Assuming the self-elastic similarity hypothesis of (McMahon and Kronauer, 1976), the heights, weights, and natural frequencies of the first mode for four species of coniferous trees, 30 samples in three categories of size including small, mid-size, and full-size trees with average heights of 0.3, 1.2 and 3.0 meters, respectively, were measured. The natural frequency of small and medium-sized categories was recorded using an accelerometer, dynamic analyzer, and frequency spectra plotter. A small silicon accelerometer with a manufacturer-reported bias of ± 0.1% was used for small and medium-sized model testing. The natural frequency of the first mode of vibration was clearly defined in the spectrum by shaking models from side to side. The recordings were started when the models were released from loading and were allowed to freely vibrate. Figure 1 shows a plot of the natural frequency spectrum for the medium-sized Austrian pine tree No. AP1 is listed in Table 1. The average of five excitations was used to mark the first and second modes of vibration. Similar plots were recorded for all the small and medium-sized samples and species which are reported in Table 1. The frequency spectrum for the model support was recorded before testing any of the models to avoid any confusion in later analysis of the spectra. In general, the second mode of the natural frequencies was damped much faster than the first mode due to its interaction with the vibration of the tree's laterals. Although the second mode of vibration was not taken into account for the analysis in this study, future work is needed to ascertain its lack of importance. Within the tested species, cedar had a better response and clearer distribution between the first and second modes of vibrations compared to the

others. Spruce had the least distinct response and the highest damping.

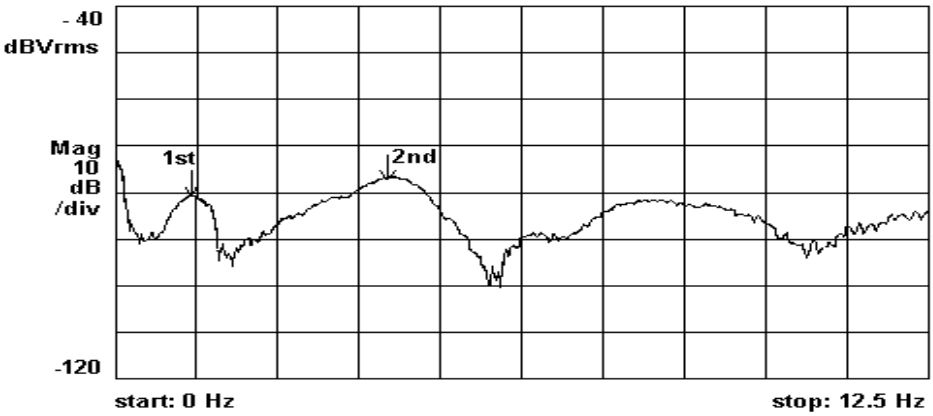

Figure 1. The frequency spectrum of medium-sized Austrian pine tree No. AP1. recorded by a dynamic analyzer.

Full-size trees with an average height of approximately 3.0 meters were only tested for their first mode of vibration. A silicon micro-machined accelerometer Model 3145 with a standard range of ±2 g and 2-volt output (i.e. precisely 988 mv/g), stable up to a frequency of 250 Hz, and a manufacturer-reported bias of ±0.2% was used for full-size tree measurements. The accelerometer was attached to the top half of the main stem. Trees were fixed at their base and were shaken from side to side at the top of the tree. The sinusoidal vibration of the shaken trees was converted to an output signal by the accelerometer, amplified ten times, and recorded. The high frequency of data acquisition (one hundred readings per second) provided a smooth sinusoidal graph and the number of swings per second could be easily determined. Thus an estimate of the first mode of the resonant frequency was found. Fig. 2 shows a plot of the natural frequency of the first mode for a full-size spruce tree No. 5. The average of three excitations (as shown in Fig. 2) was used to calculate the frequency of the first mode of vibration. Similar plots were recorded for other full-size trees as reported in Table 1.

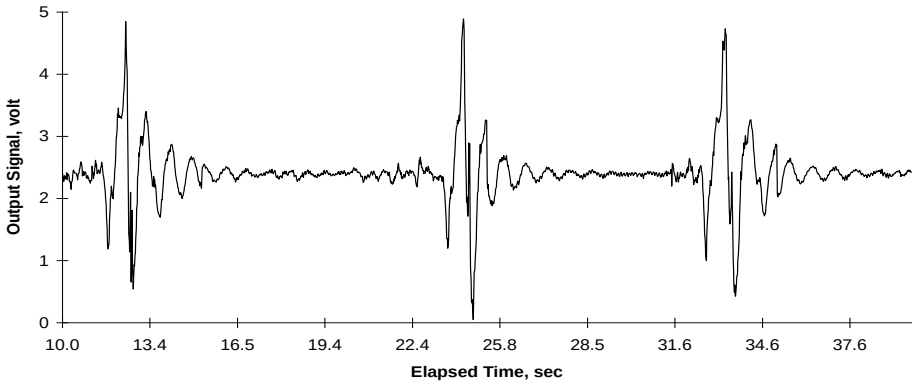

Figure 2. The output signal of the natural frequency of the first mode for full-sized spruce tree No. 5.

Table 1. Physical properties and indices (ξE) of coniferous trees.

General size	Tree species	Sample name	Height (h), m	Weight (W), N	Mass (m), Kg	m_s Kgm^{-1}	1st mode N_f, sec^{-1}	2nd mode N_f, sec^{-1}	Index ξE Nm^{-2}	Average ξE Nm^{-2}
Small size models	Cedar	C93	0.3	1.03	0.10	0.35	3.75	15.5	4.90	4.90
	Aus. Pine	AP93	0.3	1.27	0.13	0.43	4.00	19.75	6.92	6.92
mid-size models	Cedar	C1	1.40	17.50	1.78	1.27	1.38	3.75	2.41	1.97
		C2	1.15	8.62	0.88	0.76	1.63	5.00	2.02	
		C3	0.85	4.19	0.43	0.50	1.73	5.25	1.49	
	Spruce	S1	1.55	22.02	2.25	1.45	1.65	3.38	3.94	3.25
		S2	1.25	16.82	1.72	1.37	1.60	4.00	3.51	
		S3	0.65	4.91	0.50	0.77	1.73	12.50	2.30	
	Aus. Pine	AP1	1.25	25.60	2.61	2.09	1.13	4.25	2.64	3.91
		AP2	1.15	18.79	1.92	1.67	1.38	4.25	3.15	
		AP3	0.75	8.65	0.88	1.17	2.25	7.75	5.95	
Full-size trees	Cedar	CW1	2.95	62.07	6.33	2.14	1.05	-	2.34	2.11
		CW2	3.30	83.40	8.50	2.58	1.02	-	2.68	
		CW3	3.10	83.87	8.55	2.76	0.92	-	2.35	
		CW4	2.85	51.93	5.29	1.86	1.08	-	2.17	
		CW5	2.50	33.78	3.44	1.38	1.12	-	1.73	
		CW6	2.20	31.78	3.24	1.47	1.07	-	1.67	
		CW7	1.90	28.59	2.91	1.53	1.09	-	1.81	
	Spruce	SW1	3.45	103.59	10.56	3.06	1.10	-	3.67	3.41
		SW2	2.35	46.30	4.72	2.01	1.43	-	4.11	
		SW3	3.15	81.36	8.29	2.63	1.13	-	3.33	
		SW4	2.65	40.22	4.10	1.55	1.24	-	2.39	
		SW5	3.85	267.81	27.30	7.09	0.71	-	3.57	
	White Pine	WPW1	2.80	102.42	10.44	3.73	0.86	-	2.73	2.99
		WPW2	2.15	86.29	8.80	4.09	0.92	-	3.43	
		WPW3	1.90	54.58	5.56	2.93	0.98	-	2.81	
	Aus. Pine	APW1	2.95	116.44	11.87	4.02	1.09	-	4.78	5.02
		APW2	3.20	133.30	13.59	4.25	0.94	-	3.75	
		APW3	3.10	149.83	15.27	4.93	1.05	-	5.43	
		APW4	3.25	186.80	19.04	5.86	1.02	-	6.10	

3. Results and discussion

The measured height, mass, natural frequency, and the calculated index (ξE) from Eq. 2 is recorded in Table 1 for each tested sample. A simple averaging technique was applied first to the calculated indexes (ξE) of each species in each category of sizes and then over the size categories. The resulting representative indexes are 2.07, 3.36, 2.99, and 4.54 $N\,m^{-2}$ for cedar, spruce, white pine, and Austrian pine trees, respectively. In a relative sense, the representative indexes are in agreement with the reported value of the modulus of elasticity (E) in (Niklas, 1992). The Austrian pine and cedar have the maximum and minimum rigidity respectively, while the white pine and spruce are in the medium range of rigidity within all species of coniferous trees. It should be noted that because the small-sized models of cedar

and Austrian pine were low in number (Table 1), they were not used in the averaging for calculations of the representative indexes.

3.1. Validation of presented tree indices

A mathematical model has been developed by Fathi-Moghadam (Fisher and Dawson, 2003) to estimate the resistance coefficients (coefficients of drag and energy) for flow through coniferous trees. The model is based on a dimensional analysis supported by a series of experiments. Using the mathematical model, the relationship between correlated energy coefficient (*f*) and average flow velocity for four species of coniferous trees (cedar, spruce, white pine, and Austrian pine) are shown in Fig. 3. The curves in this figure are averages of testing five samples for each species of coniferous trees. A noticeable difference in energy coefficient (*f*) from one species to another in Fig. 3 may lead to criticism of the application of this single mathematical model for all species of evergreen trees. However, the difference in energy coefficient in Fig. 3 is due to variations in shape, leaf density, and material properties, which are entirely accounted for by the tree index (ξE).

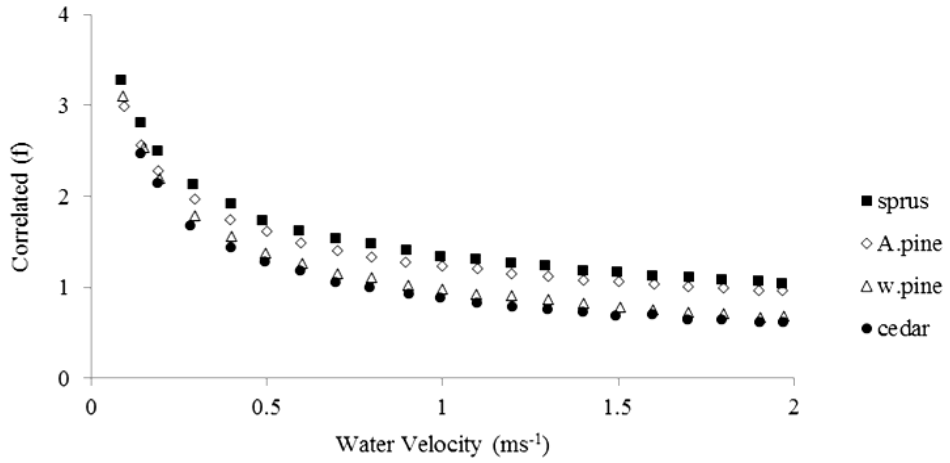

Figure 3. Correlation of energy coefficient (*f*) and flow velocity (*V*) for four species of coniferous trees

In order to verify the representative vegetation indices (ξE), the average flow velocity (*V*) in the x-axis of Figure 3 is normalized by the indices for each tested tree species in the form of $V\rho^{0.5}\left(\xi E\right)^{-0.5}$, where ρ is the mass density of the fluid ($Kg\ m^{-3}$). Using unit mass density for the same fluid flow, the resulting relationships are plotted in Fig. 4 for all tree species tested in this study. As was expected, the best-fit curves for each species in Fig. 4 are approximately 50% closer together than those in Fig. 3. This will allow the curves to be combined for an average curve (coniferous index curve) that represents the physical behavior of most species of coniferous trees. The final result of a linear regression of the data for water flow through coniferous trees is:

$$f = 2.98\left[V\rho_a^{\,0.5}\left(\xi E\right)^{-0.5}\right]^{-0.46} \quad (3)$$

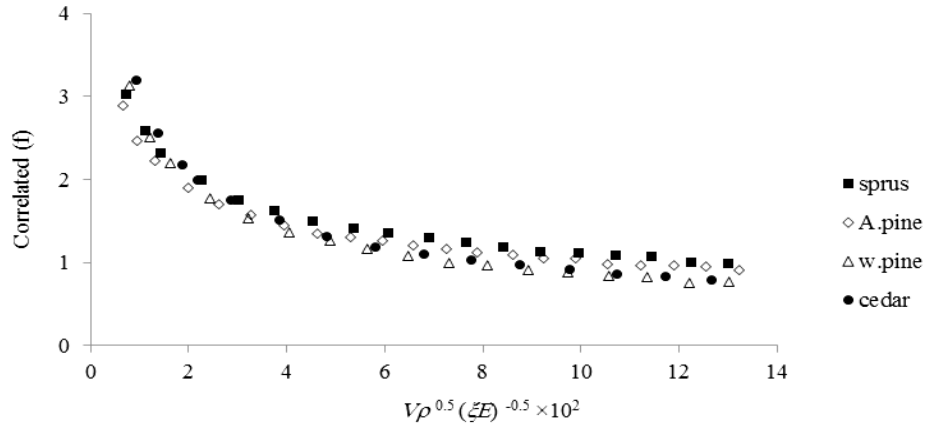

Figure 4. Correlation of energy coefficient (f) and normalized $\left[V\rho_a^{0.5}\left(\xi E\right)^{-0.5}\right]$ for four species of coniferous trees.

Eq. (3) can be used to estimate the energy coefficient (f) for water flow through coniferous trees in forest canopies. Using principles of fluid mechanics, the drag coefficient and reacted force by trees are calculated. Similar power functions between f and V as in Eq. 3 were suggested in the literature (Freeman et al., 2000) for water flow through a stand of trees on flood plains or in vegetated zones of rivers. However, no index or practical method has been proposed to account for the effect of type and variation of vegetation on the energy coefficient.

3.2. Relationship between height and natural frequency

In practice, Eq. (1) is not an exact relationship because damping is not considered. damping of vibration is not negligible even for homogeneous metal materials. For a highly damped, non-homogeneous, and visco-elastic tree, a relationship between the height (h) and natural frequency of the first mode (f_1) can only be empirically based on a large number of experimental data.

Figure 5 shows a graphical relationship between the height and the natural frequency of the first mode for the whole range of heights (0.3-3.85 m) and tree species tested in this study (Table 1). An overall linear logarithmic fitting between the (f_1) and the (h) for all the data results in the following relationship:

$$f_1 = 1.81(h)^{0.58} \tag{4}$$

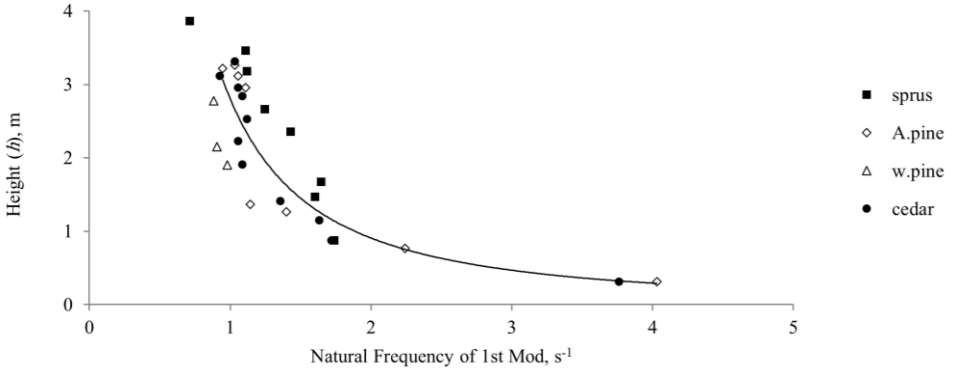

Figure 5. Relationship between natural frequency of first mode and height of trees.

Since Eq. (4) is based on the data of four species of coniferous trees, it cannot be used to estimate the (f_1) in Eq. (2) for a particular species other than coniferous trees. As (Tsujimoto et al., 1991) showed that simulated grass sway at low frequencies and suggested a power function represented by $f_1 \propto h^{-0.5}$, many more tree species should be tested in order to develop a more general relationship between the natural frequency and tree height of different species.

4. Conclusions

The physical properties of trees have a notable influence on their reaction and resistance to water flow and the rate of exchange of momentum and energy between vegetation canopies and river flow. In the present study, a method was developed to index the physical behavior of tree species and to account for the effect of tree conditions and properties (i.e. leaf density, shape, stiffness, and manner of deflection) on the drag and energy transfer coefficients. The presented trees' indices (ξE) were used to normalize flow velocity, which enables the elimination of coefficient variations among different species of coniferous trees. A single correlation between the energy coefficient and the normalized flow velocity results in a single mathematical model for various species of coniferous trees. The trees' indices were shown to be adequately capable of differentiating between tree species and conditions in the mathematical model. Using the trees' indices, the model estimated energy coefficients for coniferous trees were consistent with the reported coefficients by Järvelä (2002) for willows. In the future, estimation of the innovative index (ξE) for each tree species will require extensive sampling and testing of trees having a greater variety in appearance and physical characteristics. Assuming availability of indices for different tree species, correlating the ground-based measurements and high-resolution satellite data will analyze large forest areas possible (Rautiainen et al., 2003; Stenberg et al., 2003).

Data Availability

The data used to support the findings of this study is available from the corresponding author upon request.

Conflicts of Interest

The authors declare that they have no conflicts of interest regarding the publication of this paper.

Acknowledgments

The author acknowledges the Shahid Chamran University of Ahvaz, Ahvaz, Iran for financial support of the research.

References

Aberle, J., Järvelä, J., 2013. Flow resistance of emergent rigid and flexible floodplain vegetation. Journal of Hydraulic Research, 51(1): 33-45.

Chenge, I.B., 2021. Height–diameter relationship of trees in Omo strict nature forest reserve, Nigeria. Trees, Forests and People, 3: 100051.

Clough, R.W., Penzien, J., 2003. Dynamics of structures. Berkeley. CA: Computers and Structures.

Fang, Z., Gong, C., Revell, A., O'Connor, J., 2022. Fluid–structure interaction of a vegetation canopy in the mixing layer. Journal of Fluids and Structures, 109: 103467.

Fathi-Moghadam, M., Yarahmadi, M., Bajestan, M., 2010. Effects of land slope and flow depth on retarding flow in gravel-bed lands. Middle East Journal of Scientific Research, 5(6): 464-468.

Fisher, K., Dawson, H., 2003. Reducing uncertainty in river flood conveyance. Roughness review.

Freeman, G.E., Rahmeyer, W.H., Copeland, R.R., 2000. Determination of resistance due to shrubs and woody vegetation.

Gosselin, F.P., 2019. Mechanics of a plant in fluid flow. Journal of Experimental Botany, 70(14): 3533-3548.

Järvelä, J., 2002. Flow resistance of flexible and stiff vegetation: a flume study with natural plants. Journal of hydrology, 269(1-2): 44-54.

Järvelä, J., 2004. Determination of flow resistance caused by non-submerged woody vegetation. International Journal of River Basin Management, 2(1): 61-70.

Ji, U., Järvelä, J., Västilä, K., Bae, I., 2023. Experimentation and Modeling of Reach-Scale Vegetative Flow Resistance due to Willow Patches. Journal of Hydraulic Engineering, 149(7): 04023018.

Kafuti, C. et al., 2022. Height-diameter allometric equations of an emergent tree species from The Congo Basin. Forest Ecology and Management, 504: 119822.

Kouwen, N., Fathi-Moghadam, M., 2000. Friction factors for coniferous trees along rivers. Journal of hydraulic engineering, 126(10): 732-740.

Makowski, M. et al., 2019. Synthetic silviculture: Multi-scale modeling of plant ecosystems. ACM Transactions on Graphics (TOG), 38(4): 1-14.

McMahon, T.A., Kronauer, R.E., 1976. Tree structures: deducing the principle of mechanical design. Journal of theoretical biology, 59(2): 443-466.

Mewis, P., 2021. Estimation of vegetation-induced flow resistance for hydraulic computations using airborne laser scanning data. Water, 13(13): 1864.

Moreno-Fernández, D. et al., 2018. National-scale assessment of forest site productivity in Spain. Forest Ecology and Management, 417: 197-207.

Niklas, K.J., 1992. Plant biomechanics: an engineering approach to plant form and function. University of Chicago press.

Niklas, K.J., Moon, F.C., 1988. Flexural stiffness and modulus of elasticity of flower stalks from Allium sativum as measured by multiple resonance frequency spectra. American Journal of Botany, 75(10): 1517-1525.

PUGSLEY, A., 1988. Limits to size set by trees. Structural (The) engineer. Part A: the journal of the Institution of Structural Engineers-monthly, 66(19): 322-323.

Rautiainen, M., Stenberg, P., Nilson, T., Kuusk, A., Smolander, H., 2003. Application of a forest reflectance model in estimating leaf area index of Scots pine stands using Landsat-7 ETM reflectance data. Canadian journal of remote sensing, 29(3): 314-323.

Stenberg, P., Nilson, T., Smolander, H., Voipio, P., 2003. Gap fraction based estimation of LAI in Scots pine stands subjected to experimental removal of branches and stems. Canadian Journal of Remote Sensing, 29(3): 363-370.

Timoshenko, S.P., Gere, J.M., 2009. Theory of elastic stability. Courier Corporation.

Tsujimoto, T., Kitamura, T., Okada, T., 1991. Turbulent structure of flow over rigid vegetation covered bed in open-channel KHL Progressive Report 7, Hydr. Lab., Kanazaw a University, Japan.

Tymiński, T., Kałuża, T., 2012. Investigation of mechanical properties and flow resistance of flexible riverbank vegetation. Polish Journal of Environmental Studies, 21(1): 201-207.

van Wesenbeeck, B.K. et al., 2022. Wave attenuation through forests under extreme conditions. Scientific reports, 12(1): 1884.

Wang, H.-C., Worley, W.J., 1966. Tables of natural frequencies and nodes for transverse vibration of tapered beams.

Wang, J., He, G., Dey, S., Fang, H., 2022. Influence of submerged flexible vegetation on turbulence in an open-channel flow. Journal of Fluid Mechanics, 947: A31.